A rapid field-use assay for mismatch number and location of hybridized DNAs†

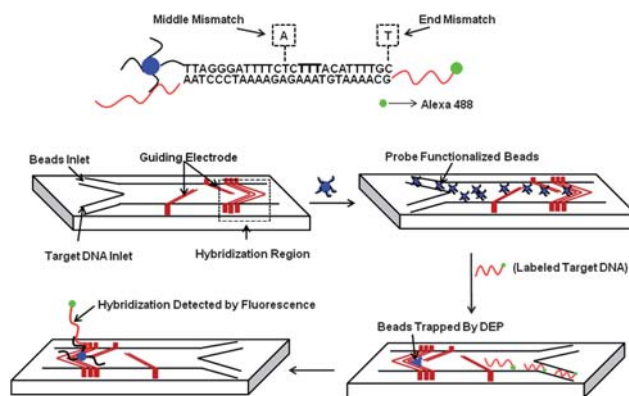I-Fang Cheng,[a] Satyajyoti Senapati,[b] Xinguang Cheng,[b] Sagnik Basuray,[b] Hsien-Chang Chang[a] and Hsueh-Chia Chang*[b]

Molecular dielectrophoresis (DEP) is employed to rapidly (<ms) trap ssDNA molecules in a flowing solution to a cusp-shaped nanocolloid assembly on a chip with a locally amplified AC electric field gradient. By tuning AC field frequency and DNA DEP mobility relative to its electrophoretic mobility due to electrostatic repulsion from like-charged nanocolloids, mismatch-specific binding of DNA molecules at the cusp is achieved by the converging flow, with a concentration factor about 6 orders of magnitude higher than the bulk, thus allowing fluorescent quantification of concentrated DNAs at the singularity in a generic buffer, at room temperature within a minute. Optimum flow rate and the corresponding hybridization rate change by nearly a factor of 2 with a single mismatch in the 26 base docking sequence and are also sensitive to the mismatch location. This dielectrophoresis and shear enhanced pico-molar sensitivity and SNP selectivity can hence be used for field-use DNA detection/identification.

The potential use of a genetic approach for the detection of micro-organisms has created an urgent need to develop a rapid, portable and highly sensitive DNA hybridization assay platform for point-of-need or field applications.[1–3] A major challenge for the portable DNA detection is the development of detection devices that neither use sophisticated instruments nor reagents. Another requirement is to eliminate the repeated washing steps in current assays to prevent non-specific binding. Differentiating a target DNA sequence from its congeneric sequence with only a few mismatches or identifying a mutation with SNP represent the most stringent selectivity and specificity metrics for field-use assays.[4,5] Commonly used DNA hybridization detection protocols, such as Southern blot and micro-array techniques, use complicated protocol and instrumentation and rely on surface bound hybridization, which makes both techniques too slow for field applications due to transport-limiting kinetics.[6,7]

Here we show an open flow-based rapid, simple, specific, and sensitive microfluidic detection platform that detects the DNA hybridization within a minute, without repeated rinsing/washing, heating and complicated hybridization buffers in its detection

protocol (Scheme 1). It also offers pico-molar sensitivity, which is adequate for most field applications, even though the resolution is lower than the most sensitive lab-based fluorescent assays with confocal detection. This simple microfluidic platform operates by dielectrophoretic (DEP) trapping of 26 base sequence probe functionalized on 500 nm silica nanocolloids in a microfluidic platform coupled with a fluorescence detector and is used to perform DNA hybridization detection of fluorescently labeled target oligonucleotides using diluted 0.08X PBS at room temperature. This approach is very sensitive and specific to mismatch discrimination and also the location of mismatches present in the 26 bases of the target DNA hybridization region. The optimum flow rate provides high shear-enhanced discrimination between target DNA sequence and a single mismatch sequence, as well as continuously removing any non-specifically bound molecules. With the nanocolloid assembly focusing the electric and flow fields, the fluorescently labeled target nucleotides in the injected solution are trapped and concentrated at the cusp of the probe functionalized nanocolloid assembly in the chip (Scheme 1). The cusp shaped geometry of the nanocolloid assembly produces a large positive field gradient that helps to trap the target DNAs. This allows rapid hybridization and accumulation of detectable fluorescence intensity in less than a minute at 100 pM target DNA concentration. The nanocolloid assembly facilitates high detection sensitivity as it provides high surface to volume ratio for DNA hybridization[8,9] and amplifies the electric field provided by microelectrodes to enhance the dielectrophoretic molecular trapping rate. The open-flow platform enhances detection sensitivity by filtering a low number of target molecules from a large sample volume, thus improving detection sensitivity to pico-molar levels, and SNP-discriminating selectivity with its high shear-rate. With the long-range dielectrophoretic trapping force, the nanocolloid assembly

[a]Institute of Nanotechnology and Microsystems Engineering, Institute of Biomedical Engineering, Center for Micro/Nano Science and Technology, National Cheng Kung University, Tainan, Taiwan, ROC
[b]Center for Microfluidics and Medical Diagnostics, Department of Chemical and Biomolecular Engineering, University of Notre Dame, Notre Dame, 46556, IN, USA. E-mail: hchang@nd.edu; Fax: +574-631-8366; Tel: +574-631-5697
† Electronic supplementary information (ESI) available: Supplementary Materials and Methods, and videos I and II. See DOI: 10.1039/b925854j

Scheme 1

needs only to occupy a fraction of the flow channel and hence offers very little hydrodynamic resistance. A large throughput is possible with simple sample injection instrumentation like a hand-held syringe. The linear velocity at a typical operating flow rate of 1 µL/min is estimated to be 1.7 mm/s producing a transit time of 1.8 ms of the solution across the 30 micron nanocolloid assembly. The enhanced DEP DNA mobility can hence trap each molecule to the assembly within 1 ms. The minute-long detection time is determined by how many target molecules can be trapped from the flowing sample solution before the detection threshold is reached.

In contrast, traditional batch DNA hybridization protocols require an hour-long detection time with stringent hybridization conditions, low ionic strength buffer solution and high temperature, which allow only homologous sequences to hybridize with target DNA molecules.[10] The employment of certain cations in the hybridization buffer overcomes the repulsion between complementary strands that helps to prevent degradation of the oligonucleotide sequence and also enables the recognition of complementary bases.[11] Our platform eliminates these hybridization requirements as it employs dielectrophoresis to overcome repulsive probe–target interaction—in fact, balancing the two forces such that the target molecules do not foul the entire nanocolloid array but rather concentrate at its tip, thus

achieving rapid concentration and hybridization of DNA molecules before its degradation and attaining high specificity by shearing off any non-specifically bound oligonucleotide sequences or other non-target molecules. Hence, no washing step is required in our platform unlike in conventional assays. Our platform uses buffer solution with an ionic strength 10 times lower than the traditional hybridization protocols, thus enhancing the specificity further with electrostatic repulsion. Detailed procedures for chip fabrication and on-chip DNA hybridization assay are provided in the ESI.†

We observed that at high target DNA concentrations ($\geq$ 100 pM) the fluorescence intensity starts to appear within 30 s which is clearly indicative of rapid hybridization of target species with the functionalized probe on the nanocolloid surface [Fig. 1 (a and c)]. However, at low target DNA concentration ($\leq$ 1 pM), the detectable fluorescence intensity takes longer to appear. It is estimated that $\sim$10^6 fluorescently labeled target DNA molecules are required to concentrate in the micron-sized cusp region of the nanocolloid assembly to achieve detectable fluorescence intensity for our detection imaging system. The hybridization rate is found to be sensitive to the frequency within a window of 800 kHz to 1.2 MHz. Beyond this frequency window, the detection of DNA hybridization is about 2–3 times slower (Fig. 1a). The delayed appearance of detectable threshold
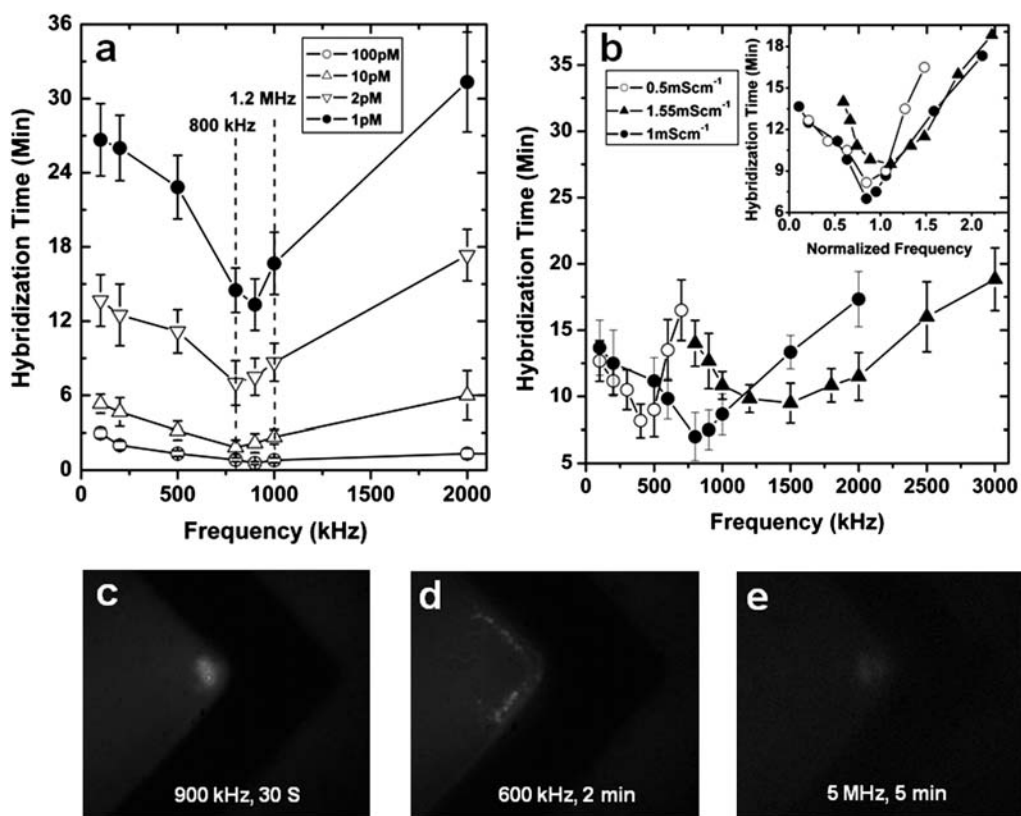

Fig. 1 (a) The effect of frequency with hybridization time as a function of target DNA concentration. Dotted lines represent the optimum frequency window to obtain maximum hybridization efficiency with our detection platform. (b) The effect of frequency with hybridization time as a function of conductivity of the buffer solution at 1 pM DNA concentration. The inset in (b) represents a plot of optimum frequency scaled by D/λ^2, where D is diffusivity of DNA [D for 300 bases of oligonucleotide is 2×10^{-11} m^2 s^{-1} ref. 18] and λ is length of Debye double layer (5.32 nm, 3.76 nm and 3.1 nm for the three PBS buffers at 0.5 mS/cm, 1 mS/cm and 1.55 mS/cm respectively). (c–e) Image of the trapped bead region near the convergent electrode area when the hybridization reaction is performed with 100 pM target DNA solution (c) in the observed frequency window (ω = 900 kHz), showing a high intensity of fluorescence at a localized area, confirming DNA hybridization after 30 s (d) below the observed frequency window (ω = 600 kHz) showing fluorescence intensity from a dispersed area after 2 min. (e) Above the observed frequency window (ω = 5 MHz) showing much less hybridization. The ssDNA used is the same as in our earlier publication (ref. 7).

fluorescence intensity outside this frequency window suggests that target DNA molecule concentrates at a much slower rate at these frequencies. The DEP force on the DNA molecules is hence a strong function of the applied AC electric field frequency. This frequency window is not very prominent at high concentration ($\geq$ 100 pM), as it is difficult to determine the change in fluorescent intensity with time as a large number of fluorescently labeled target molecules reach the hybridization site rapidly (Fig. 1a). At lower DNA concentrations (1 pM), we find that this frequency window is also a strong function of conductivity of the medium (Fig. 1b). The frequency window shifts to higher frequency region as the conductivity of the hybridization medium increases. We will show that the frequency window arises due to interplay between dielectrophoretic force and electrostatic repulsive force between the negatively charged nanocolloids surface and negatively charged DNA back bone.

Dielectrophoresis occurs when a field-induced dipole is endowed on the target DNA. Earlier experiments on dsDNA[12,13] show that there is a frequency window for which the molecule exhibits positive dielectrophoresis—they are attracted to the high field region in the crevices of the nanocolloid assembly. Further, the intensity of the electric field is very sensitive to the electrode geometry.[14] The field across our micro-electrode pair and at the convergence region are $\sim 2 \times 10^6$ V/m and $\sim 1 \times 10^7$ V/m respectively and we expect an amplification factor of 10 to 100 by the nanocolloid assembly. Since the dielectrophoretic force and velocity scales quadratically with respect to the field, the molecular DEP force at our nanocolloid assembly is about 3–4 orders higher than the earlier experiments,[12,13] or $\sim 10^{-11}$ N and is comparable to the hydrodynamic Stokes drag on a 1 kb ssDNA in coiled conformation. The upper bound of the positive dielectrophoresis frequency window corresponds to the inverse polarization time of the molecule.[15,16] As was shown recently with macro-ions, the lower frequency bound corresponds to the inverse relaxation time of the screening macro-ions onto the electrode or the high-field region.[17] Below this frequency, the macro-ions adsorb onto the high-field region and screen the field to prevent appreciable molecular dielectrophoresis. This lower bound on positive molecular dielectrophoresis occurs at the inverse relaxation time of the macro-ion molecule D/λ^2 where D is the diffusivity of the molecule and λ the Debye double layer length.[18,19] For smaller nanocolloids and biological molecules, the dielectric force is a strong function of surface characteristics and double layer conductance.[18,19]

In the context of earlier work on molecular and macro-ion dielectrophoresis, we interpret the observed frequency window in rapid hybridization of DNA in our open flow-based microfluidic platform with the following mechanism. At low frequency (ω <800 kHz), the high positive dielectrophoretic force on DNA molecule overcomes the electrostatic repulsive force between negatively charged nanocolloid and the negatively charged phosphate backbone on DNA molecules. This allows the DNA molecules to come close to the nanocolloid surface, which results in the non-specific adsorption or hybridization of the DNA molecules onto the outer boundary of the entire nanocolloid assembly (Fig. 2a) (see video-I in the ESI†). This global coverage of the nanocolloid assembly prevents further molecular trapping and prevents the concentration of DNA molecules at the cusp of the nanocolloid assembly (Fig. 1d). On the other hand, at high frequency (ω > 2 MHz), molecular polarization and dielectrophoretic force become negligible and the repulsive bead-DNA electrostatic force dominates (Fig. 2b), resulting in negligible hybridization of DNA even after passing target DNA through the
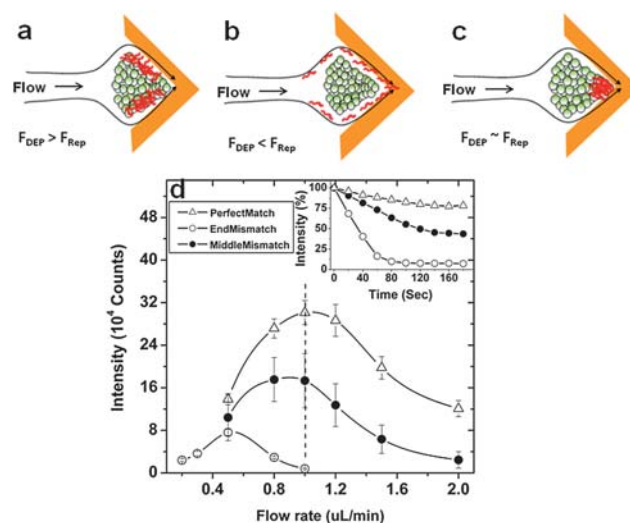

Fig. 2 Schematic representation of the DNA hybridization pathway through cusp-shaped nanocolloid assembly (a) at low frequency (ω < 800 kHz), (b) at high frequency (ω > 1.2 MHz), (c) at optimum frequency (800 kHz $\leq \omega \leq$ 1.2 MHz). (d) Effect of flow on DNA hybridization for perfect match, end and middle mismatch probe sequence with the mismatch corresponding to a C base replaced by a T base for end mismatch and T base replaced by an A base for middle mismatch as shown in Scheme 1. The dotted line indicates the optimum flow rate for high detection specificity of target DNA with maximum hybridization efficiency when end mismatch probe sequence is designed for SNP detection. The inset of Fig. 2d shows the change of fluorescence intensity for perfect match, end and middle mismatch probe sequence due to dehybridization of target DNA from the probe functionalized silica surface at a flow rate of 1.5 µL/min for 3 min.

trapped bead region for 5 min (Fig. 1e). In contrast, within the observed frequency window (800 kHz $\leq \omega \leq$ 1.2 MHz), both dielectrophoretic force and repulsive force are comparable. As a result, the DNA molecules are attracted to the bead surface by dielectrophoresis but do not adsorb due to electrostatic repulsion. They are then convected by surface flow to the cusp of the nanocolloid assembly (Fig. 2c) (see video-II in the ESI†). This allows high number of DNA molecules to rapidly concentrate at the cusp with maximum field and DEP force (Fig. 1c). In fact, the optimum frequency scaled by D/λ^2 (where D is the diffusivity of the 300 base[20] ssDNA at 2×10^{-11} m^2 s^{-1} and $\lambda = \sqrt{\varepsilon kT/2N_A e^2 I}$, the Debye double layer length at the given ionic strength I), can be collapsed (inset of Fig. 1b). This gives further credence to our theory that indeed the convection of the DNA molecules to the cusp requires a balance between electrostatic repulsion and dielectrophoretic forces transverse to the flow.

Our open flow-based microfluidic approach helps to distinguish between target and non-target DNA with rapid concentration buildup at the cusp by shearing off the non-target DNA while the target DNA remains bound by the functionalized probe at the nanocolloid surface by hybridization. This gives rise to very high detection specificity in our platform. To evaluate the specificity of our platform, single mismatch probe sequence having mismatches at the middle and one end of the 26 bases of hybridization region are investigated using the same target DNA sequence under identical conditions. At low flow rate of target DNA buffer solution ($\leq$ 0.5µL/min) for an end mismatch probe sequence, we observed a nearly four-fold smaller fluorescence intensity (compared to perfectly matched

probe sequence) at the trapped bead region that gradually disappears as the flow rate increases to an optimum value of 1 μL/min (Fig. 2d). This clearly demonstrates the shear discrimination of non-specifically bound target DNA molecules on the nanocolloids surface at high flow rate and thus offers high detection specificity between end mismatch probe sequence and target DNA sequence. On the other hand, the relative change in fluorescence intensity due to dehybridization of target DNA for a middle mismatch is nearly less than two times the intensity of a perfectly matched probe sequence under a similar flow rate of 1.5 μL/min (inset of Fig. 2d). The dehybridization study at constant flow rate of 1.5 μL/min clearly demonstrates that detection is very sensitive to the mismatch location. The cause of reduction in enhanced shear discrimination effect due to middle mismatch as compared to end mismatch probe sequence location is not clear. This needs to be studied in more detail to evaluate the co-relation between DNA conformations due to interplay of electric field and shear flow and mismatch location in the 26 base probe sequence. However, it is clear that the shear discrimination is easier if sequence is unzipped from one end (Fig. 2d). The fluorescence intensity of hybridization at optimum flow rate for perfect (1 μL/min) and end mismatch (0.5 μL/min) show a change of nearly a factor of 4 (Fig. 2d). Further, for a perfect matched probe sequence, the maximum hybridization efficiency is observed at a flow rate of 1 μL/min beyond which the target DNA molecules denature from the hybridized region of the bead surface (Fig. 2d). Thus, to detect SNP, the mismatch location can be designed at the end of the sequence so that high specificity and rapid hybridization can be achieved at the optimum frequency window of 800 kHz to 1.2 MHz and with the optimum flow rate of 1 μL/min. We expect that this detection platform will be useful in applications such as single polymorphism analysis, immunoassay-based pathogen detection, point-of-need and field-use applications where single-mismatch resolution, mismatch location, sensitivity, rapid detection and simplicity is the determining criterion for selection of diagnostic tools. For future work, a stationary nanocolloid assembly would remove the need of assembling the assembly each time.

Acknowledgements

Notes and references

1 E. Palecek, *Trends Biotechnol.*, 2004, **22**, 55–58.
2 G. Hutvagner, J. Mclachlan, A. E. Pasquinelli, E. Balint, T. Tuschl and P. D. A. Zamore, *Science*, 2001, **293**, 834–838.
3 J. Khandurina, T. E. McKnight, S. C. Jacobson, L. C. Waters, R. S. Foote and J. M. Ramsey, *Anal. Chem.*, 2000, **72**, 2995–3000.
4 A. J. Tüdős, G. A. J. Besselink and R. B. M. Schasfoort, *Lab Chip*, 2001, **1**, 83–95.
5 T. A. Taton, C. A. Mirkin and R. L. Letsinger, *Science*, 2000, **289**, 1757–1760.
6 J. Ng Kian-Kok, H. Feng and W. T. Liu, *Anal. Chim. Acta*, 2007, **582**, 295–303.
7 S. Basuray, S. Senapati, A. Aijian, A. R. Mahon and H.-C. Chang, *ACS Nano*, 2009, **3**, 1823–1830.
8 T. Lund-Olesen, M. Dufva and M. F. Hansen, *J. Magn. Magn. Mater.*, 2007, **311**, 396–400.
9 S. Senapati, A. R. Mahon, J. Gordon, C. Nowak, S. Sengupta, T. H. Q. Powell, J. Feder, D. M. Lodge and H. -C. Chang, *Biomicrofluidics*, 2009, **3**, 022407–7.
10 http://www.scricciolo.com/classificazione/sequence7.htm.
11 R. de la Rica, C. Ferna'ndez-Sa'nchez, C. Jime'nez-Jorquera and A. Baldi, *J. Phys. Chem. B*, 2008, **112**, 7614–7617.
12 C. L. Asbury and G. V. D. Engh, *Biophys. J.*, 1998, **74**, 1024–1030.
13 C. L. Asbury, A. H. Diercks and G. V. D. Engh, *Electrophoresis*, 2002, **23**, 2658–2666.
14 I.-F. Cheng, H.-C. Chang, D. Hou and H.-C. Chang, *Biomicrofluidics*, 2007, **1**, 021503–15.
15 C. F. Chou, J. O. Tegenfeldt, O. Bakajin, S. S. Chan, E. C. Cox, N. Darnton, T. Duke and R. H. Austin, *Biophys. J.*, 2002, **83**, 2170–2179.
16 C. F. Chou, O. Bakajin, S. W. P. Turner, T. A. J. Duke, S. S. Chan, E. C. Cox, H. G. Craighead and R. H. Austin, *Proc. Natl. Acad. Sci. U. S. A.*, 1999, **96**, 13762–13765.
17 P. Hoffman and Y. Zhu, *Appl. Phys. Lett.*, 2008, **92**, 224103–3.
18 S. Basuray and H.-C. Chang, *Phys. Rev. E: Stat., Nonlinear, Soft Matter Phys.*, 2007, **75**, 060501–060504.
19 S. Basuray and H.-C. Chang, *Biomicrofluidics*, 2010, **4**, 013205–11.
20 A. E. Nkodo, J. M. Garnier, B. Tinland, H. Ren, C. Desruisseaux, L. C. McCormick, G. Drouin and G. W. Slater, *Electrophoresis*, 2001, **22**, 2424–2432.